# Density-functional study of adsorption of isocyanides on the gold (111) surface.

Yulia Gilman
*Department of Physics and Astronomy, State University of New York, Stony Brook, NY 11794-3800*

Philip B. Allen
*Department of Physics and Astronomy, State University of New York, Stony Brook, NY 11794-3800*, and Center for Functional Nanomaterials, Brookhaven National Laboratory, Upton, New York 11973-5000*

Mark S. Hybertsen
*Department of Applied Physics and Applied Mathematics, and Center for Electron Transport in Molecular Nanostructures, Columbia University, New York, NY 10027*

Density functional theory within the generalized-gradient approximation is used to study the adsorption of the isocyanides CNH and $CNCH_3$ on the gold (111) surface at several coverages. It is found that these molecules are highly selective in their adsorption site preference. Adsorption is possible only at the top site, although binding is rather weak and dipole-dipole repulsion prevents binding at coverages of 1/3 ML and higher. At all other high symmetry sites considered (hcp, fcc, bridge), the isonitriles are not bound. To reveal the main mechanisms of bonding, the isonitriles are compared to CO and ammonia using Au-X radicals as model systems. The systematic trends are understood in terms of $\sigma$ donation from the ligand lone pair and $\pi^*$ back donation. Finally, CNH is found to be more strongly bound to an undercoordinated gold atom (adatom) on the surface.

## I. INTRODUCTION

Gold is widely chosen as an electrode material for studies of molecular conductance for a number of practical reasons, including ease of deposition and patterning and presentation of a surface that is relatively easy to clean and maintain. Another important factor has been the extensive base of experience in forming self assembled monolayers (SAMs) of organic molecules, linked to the gold surface via a sulfur atom. The initial discovery of the thiol-gold route to self assembly[1] led to rapid growth in the study of the formation and properties of organic layers[2,3]. The S-Au bond is relatively strong ($\sim$1.7 eV), but the barrier to lateral motion between adsorption sites is rather low ($\sim$0.1 eV), facilitating formation of ordered monolayers[2]. Sulfur has been alsmost exclusively used as the "alligator clip"[4] in the experiments probing conductance at the molecular scale[5,6]. However, the substantial variation in the measured conductance for basic molecules such as alkanes contacted using the Au-S link, between different groups and different measurement techniques, remains a puzzle. One possibility is sample to sample variation in the local structure of the Au-S link[7]. This is consistent with the low barriers for motion that facilitate assembly and the known mobility of Au atoms during formation of the thiol linked layer[8,9]. Also, the atomic scale structure of the interface of assembled layers with Au-S linkages has proved to be a very delicate problem for *ab-initio* methods[9], although a recent study appears to reconcile extensive data for decanethiols[10]. Overall, despite wide usage, the Au-S link displays a number of critical issues for application in molecular conductance studies. Recent research has been directed to find alternative link chemistries, e.g. Ru or Mo carbene[11,12].

An alternative link chemistry for a gold electrode that shows more selectivity in the local bonding geometry is an attractive possibility in the context of molecular scale conductance. Although Au surfaces are relatively unreactive, other candidates have been explored. A very recent study demonstrated the utility of amine terminated molecules for molecular conductance studies[13]. The Au-$NH_2$-R links proved to be flexible and reproducible. Another example, with a similar bonding character, is isocyanide (CN-R, e.g. CNH), a less-stable isomer of cyanide (NC-R, e.g. NCH). Well-established synthetic methods exist for the CN- linker with various molecules (R). Bonding to Pt or Au electrodes has been observed[14]. In contrast to the Au-S link, adsorption of isocyanide (Au-CN) linked molecules on gold surfaces is much less studied. Most experimental works on this subject consider adsorption of the molecules on gold nanoparticles[15,16,17,18]. Henderson *et al.*[19] studied the formation of self-assembled monolayers of diisocyanides on the gold (111) surface. It was concluded from reflection absorption infrared (RAIR) spectra that the molecules with rigid chains between two CN- groups (such as biphenyldiisocyanide) attach to the gold surface through only one isocyanide group while the other group remains free. Ellipsometry data indicate that in these cases, the molecular axis is perpendicular to the surface. Molecules with flexible alkyl chains can attach to the gold surface through both isocyanide groups, which makes them unlikely candidates for molecular conductance studies. The preferred adsorption site and geometry remain as unresolved questions in the literature. Angelici *et al.* observed the peak in the infrared spectra

*Permanent address.

associated with N-C stretch mode to be shifted 50-70 $cm^{-1}$ higher upon adsorption on gold powder[15,16]. They concluded that isocyanides bind to the surface at the top site. Henderson *et al.*[19] observed a similar blue shift for adsorption on the gold (111) surface, but concluded that both atop and three-fold adsorption configurations are possible.

The earliest of the few theoretical works on the adsorption of isocyanide on gold considered phenyl isocyanide attached to a single gold atom, a gold dimer and a trimer[20]. The calculations showed that for each gold cluster, the binding was to a single Au atom. Bonding motifs analogous to the bridge and hollow sites on the (111) surface were not observed. The results suggest site selectivity for the isocyanide link, although the details of the adsorption energy and the geometry on the Au(111) surface remain to be determined. Recently several groups[21,22] successfully fabricated self-assembled monolayers of various diisocyanide molecules sandwiched between two gold electrodes, and studied electrical transport through them. The impact of the isocyanide link on the conduction has received some attention from theorists as well. Conductance and voltage-current characteristics of molecules connected to metallic electrodes were calculated using combined density functional theory (DFT) and non-equilibrium Green's function methods[23]. However, the adsorption geometry was not explicitly determined by energy minimization.

This paper presents a study of the adsorption of isocyanide linked molecules on the gold (111) surface using a density functional theory (DFT) approach. We focus on the binding of the essential link element to the metal surface, considering the simplest case, a CNH molecule. Calculations performed for $CNCH_3$ confirm the results. The basic electronic structure of the CNH molecule suggests that the filled lone pair on the C atom will be available for donor-acceptor type bonding to Au complexes, in analogy with ammonia ($NH_3$) and CO. We chose to draw a comparison between CNH, CO and $NH_3$ in order to better understand the factors that affect adsorption. The case of CO has been extensively studied for many transition metal surfaces[24]. There are also recent calculations for the case of $NH_3$ on Au(111)[25]. The standard Blyholder picture[26] describes the bonding in terms of the trade-off between $\sigma$ donation from the lone pair to the metal and back donation from the metal to the empty $\pi^*$ molecular orbital. Two main themes emerge: (1) the interplay of the electronic couplings in the Blyholder picture with the corresponding charge transfers; (2) the impact of the dipole moment, both that of the molecule prior to adsorption and the induced dipole upon adsorption. In the next section, the methodology and the basic results of the DFT calculations are described. The physical interpretation of the results is discussed in Sect. III.

## II. METHODOLOGY AND RESULTS

The adsorption of the target molecules on the Au surface is studied using a computational approach based on DFT. The main calculations are done using the generalized gradient approximation (GGA) of Perdew, Burke and Ernzerhof (PBE)[27]. Different forms of GGA are widely used for metal surface and adsorption problems in order to address the large errors in adsorption energy found with the local density approximation (LDA), although the accuracy still varies with the system under study[24,28,29,30,31]. For comparison, selected calculations are also done with the LDA[32,34]. To have an initial picture of the bonding, the target molecules bonded to a single Au atom are considered using the NRLMOL DFT code[35]. For the light atoms (C, N, and H), an all electron basis is used. A slight modification[36] of norm-conserving Troullier-Martins pseudopotentials is used for gold atoms. NRLMOL uses Gaussian basis sets optimized for density-functional calculations[37]. The exponents and contraction coefficients are determined by optimizing the total energy of the free atom in the ground state. For the valence states, the number of independent contractions used (s, p, d) for each atom is as follows: H (4, 3, 1), C (5, 4, 3), N (5, 4, 3) and Au (4, 2, 4). It has been shown that these basis sets are well-converged and that they have negligible basis set superposition error. Further details of the basis sets can be found in Ref.[37]. Radicals were treated with spin-polarized, unrestricted calculations.

The adsorption on the surface was modeled with the standard scheme of a periodically repeated slab geometry. We found that the slab of four layers of gold atoms was enough to reproduce key adsorption characteristics such as the binding energy. The molecules are adsorbed on one side of the slab. For most of the calculations, the molecular structure is relaxed, with the molecular axis kept perpendicular to the surface and the Au atoms in the slab frozen at their bulk positions. Relaxation is carried out until the maximum force is less than 0.15 $eV/\mathring{A}$. For selected cases, the top layer of Au atoms was allowed to relax. We also explored bonding of CNH to an Au adatom in the hcp hollow site, allowing the adatom and the surface Au atoms to relax. Most of these calculations were done using the WIEN2k DFT code (full potential and linearized augmented plane waves[38]). For comparison, some calculations were also done with the ABINIT package[39,40], which employs a plane wave basis set and pseudopotentials. LDA calculations were done with Hartwigsen-Goedecker-Hutter (HGH) pseudopotentials[41], while GGA calculations were done with Troullier-Martins type pseudopotentials[42,43]. It was checked that the energy is converged with respect to the number of k-points as well as the size of the basis set. To facilitate analysis, the partial densities of state (PDOS) were plotted in selected cases. In the WIEN2K code, a modified tetrahedron method[44] is used for density of state calculations; the PDOSs are calculated by pro-

jecting the wave functions onto the spherical harmonic basis functions centered on the atoms in question inside a sphere centered on the atom (atomic sphere radii are 1.06 $\mathring{A}$ for Au atoms, 0.58 $\mathring{A}$ for C and N, and 0.29 $\mathring{A}$ for H).

We start by considering binding of the CNH and $CNCH_3$ molecules to a single gold atom. The binding energy of the Au atom, the gold to ligand distances, and the dipole moments of the free molecules and the molecules bound to the gold atom are reported in Table I. The results for CNH and $CNCH_3$ are very similar. For comparison, results for CO and $NH_3$ are also shown. The first step of relaxation allows only configurations with axial symmetry. The axial CO and CNH molecules are very similar in their electronic structure. The highest occupied molecular orbital (HOMO) is the lone pair on the C and there is a doubly degenerate $\pi$ bond between C and the N or O. For $NH_3$, the N lone pair is the HOMO, but there are no $\pi$ bonds. The $\sigma$ part of the interaction in all three is due to coupling of the lone pair orbital on the ligand to the $d_{z^2-r^2}$ and s states on the Au. This results in partial transfer of electron density onto the Au atom. Because the Au s state is half filled, the frontier, antibonding $\sigma$ state in the complex is also half filled. The initial ligand lone pair orbital energy is highest for $NH_3$, comparable to the Au s state, and successively lower for $CNCH_3$, CNH and lowest for CO.

The $\sigma$ donation is partially balanced by the back donation from the Au $d_{zx}$ and $d_{yz}$ into the empty $\pi^*$ doublet on the molecule for CO, CNH and $CNCH_3$. This balance is slightly different for AuCNH and $AuCNCH_3$ relative to AuCO. In the AuCO case, the C-O bond length increases by 0.004 $\mathring{A}$ relative to CO. In the AuCNH ($AuCNCH_3$) case, the C-N bond length decreases by 0.007 $\mathring{A}$ relative to CNH ($CNCH_3$). This difference suggests less $\pi^*$ back donation in the AuCNH case. The reduced back donation is consistent with the $\pi^*$ doublet being about 1 eV higher in CNH and even a bit higher for $CNCH_3$. This is also consistent with the trend of increasing Au-C bond length from AuCO to AuCNH to $CNCH_3$. The trend for net charge transfer to the Au as measured by Mulliken type analysis is consistent with larger $\sigma$ donation and smaller $\pi$ back donation from $AuCNCH_3$ to AuCNH to AuCO. The binding energy follows the same order, but the impact of larger $\sigma$ donation and smaller $\pi^*$ back donation are competitive, with the $\sigma$ donation dominating the trend. By comparison, the $NH_3$ molecule shows the strongest $\sigma$ donation, with the largest charge transfer to Au, but offers no empty $\pi$ space for back donation. Its binding energy to a gold atom is 0.60 eV, less than for CO. Correspondingly the Au-N bond length is substantially larger (2.277 $\mathring{A}$). The role of the $\pi$ states is further highlighted by the results of full relaxation, which leads to bent structures for Au-CNH, Au-$CNCH_3$ and Au-CO. This bending is due to the pseudo Jahn-Teller effect. The lowered symmetry allows mixing between the half occupied $\sigma$ antibonding level in the complexes and one of the empty $\pi^*$ states. The resultant energy gain depends on the gap between $\sigma$ and $\pi^*$ states. It is largest for the Au-CO complex and smallest for Au-$CNCH_3$; the Au-CO complex has the smallest gap between $\sigma$ and $\pi^*$ states, while Au-$CNCH_3$ has the largest.

In comparison to CO, a key difference is that CNH and $NH_3$ have a much larger dipole moment. Table 1 shows the calculated dipole moments which agree well with the measured values. In all three cases, there is a substantial increase in the dipole of the gold-ligand complex relative to the isolated ligand. The dipole moment of the AuCO complex is 1.6 D for the linear configuration, compared to the small dipole of the CO molecule. The dipole of the AuCNH complex increases by 2.4 D over the CNH ligand, while the increase is 3.2 D for the $NH_3$ case. The increase in dipole can not be simply seen in a point charge approximation with associated charge transfer (e.g. from a Mulliken type analysis). Instead, the extension of the lone pair electrons at the C end of the ligand onto the Au by quantum mechanical mixing with the Au s state is responsible, partly balanced by the $\pi^*$ back donation. The reduced back donation in the AuCNH case results in a larger change in dipole. In the $NH_3$ case there is no back donation and the dipole change is even larger. On the other hand, the distortion to the bent form in the Au-CNH and Au-CO cases results in a much reduced dipole, consistent with the enhanced back donation from the Au to the C.

In addition to the hybridization considerations, the dipole also influences the relative binding of Au to the ligands. There is an additional attraction in the Au-CNH complex due to polarization of the Au by the dipole. This influences the differences in binding energy, in addition to the systematic hybridization differences. To estimate this contribution, we use the calculated polarizability of the Au atom[25] together with a point charge model of the molecule derived from fitting to the self consistent electrostatic potential and the calculated dipole moment. For the case of AuCNH, we estimate that polarization contributes 0.1 eV to the binding energy. For $AuNH_3$, the effect is even smaller (0.01 eV).

So far as we know, there are no direct measurements of the Au binding energy in these radicals. The Au-$NH_3$ radical was studied using both DFT approaches and quantum chemistry approaches for evaluation of the correlation energy (e.g. coupled cluster with singles, doubles and triple corrections, CCSD(T))[45]. Substantial care was also taken to account for basis set superposition errors, which can be a significant issue for these correlation techniques in particular[46]. The Au binding energy in this case was deduced to be 0.78±0.06 eV, similar to the GGA-PBE value we obtain. There are several studies of the Au-CO radical with DFT and quantum chemistry approaches[47,48,49,50]. Our result for the lowest energy geometry, the bent form, agrees reasonably well with previous values based on DFT with GGA: 0.71 eV[48] and 0.80 eV[50]. However, the correlated electron calculations consistently give smaller binding energies, ranging from 0.14 to 0.56 eV depending on the details[47,49]. Given con-

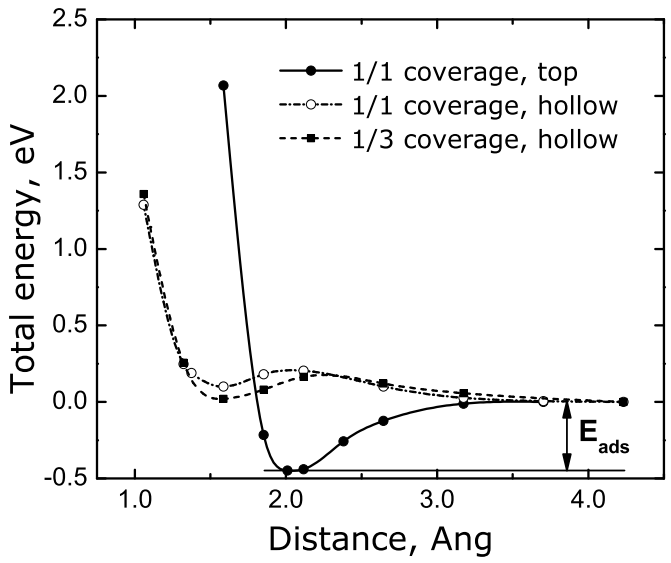


FIG. 1: Total energy (GGA-PBE) per unit cell for HNC monolayers with 1/1 and 1/3 coverages on the gold slab *vs.* distance $d$ to the surface. Molecules are at the top or filled hollow site with molecular axis perpendicular to the surface. The indicated adsorption energy is relative to a uniform molecular layer well separated from the surface.

cerns about basis set superposition errors, it is premature to draw a final conclusion from the quantum chemistry calculations in this case.

Turning to the adsorption on the surface, we initially consider a full monolayer of CNH adsorbed on one side of a slab of four gold layers. The supercell contains one molecule and four gold atoms, two of them being surface atoms. First, the molecules are placed at the top site (above the surface Au atom) and the distance from the carbon atom to the surface is varied. The molecular axis is kept perpendicular to the surface. The observed dependence of total energy *vs.* distance $d$ is shown in Fig.1. The binding energy $E_{ads}$ is the energy per molecule required to separate the layer of CNH from the Au (111) surface, leaving the free standing CNH layer otherwise unchanged. The value of $E_{ads}$ is found to be 0.43 eV and the optimal distance is 2.01 $\AA$. In order to check that four layers of gold are enough to represent the surface, we repeated the calculation for three, five, and six gold layers in the slab. The results value of $E_{ads}$ varies from 0.453 to 0.431 eV, indicating that the choice of four layers is justified.

When a molecule is placed at the filled (hcp) hollow site, the energy *vs.* distance (see Fig. 1) is qualitatively different from that at the top site. Although there is a local minimum at around 1.6 $\AA$, the energy is minimal when the molecule is far away from the surface. This indicates that the CNH molecule cannot be stabilized at the hollow hcp site. The same result is obtained for the empty hollow (fcc) and for the bridge sites.

The next candidate for a stable configuration at uniform commensurate coverage is a monolayer with one molecule per three surface atoms, forming a $\sqrt{3} \times \sqrt{3}R30^\circ$ equilateral triangular lattice on the surface, where R=2.883 $\AA$ is the distance between nearest neighbor gold atoms. The distance between molecules in this case is 4.944 $\AA$. For the CNH molecules positioned at the top site, we relax the monolayer keeping the molecular axis normal to the surface and gold atoms frozen. The adsorption energy is found to be 0.18 eV relative to the separated slab-monolayer system. For the hcp site and $\sqrt{3} \times \sqrt{3}R30^\circ$ surface unit cell, similar to the $1 \times 1$ case, the energy is minimal when molecules are far away from the surface, although there is a local minimum in energy curve (see Fig. 1). This shows that adsorption is not possible at the hcp site. Similar results are obtained for the CNH monolayer with 1/4 coverage ($2 \times 2$ surface unit cell) and the $CNCH_3$ monolayer with 1/3 coverage (see Table II).

So far binding of pre-formed monolayers was considered. For adsorption from the gas phase, the energy cost of forming the free monolayer must be taken into account. The CNH molecule has a large dipole moment, as noted above. In the case of 1 ML coverage the distance between molecules in the monolayer is 2.883 $\AA$. The point dipole approximation gives a crude estimate of about 1.4 eV per molecule for the energy cost of monolayer formation. This is much larger than the energy gained upon adsorption. Therefore HNC molecules cannot adsorb on the (111) gold surface at 1 ML coverage. For smaller coverages (1/3 and 1/4 ML) the distance between molecules is large enough for the point dipole approximation to be accurate. We calculate an energy cost of 0.26 eV per molecule to form a CNH monolayer at 1/3 ML coverage and 0.17 eV at 1/4 ML coverage. When compared to the adsorption energies in Table II, the formation of 1/3 ML is endothermic, while the 1/4 ML coverage is slightly exothermic, about 0.03 eV per molecule.

Just as noted for the AuCNH complex, adsorption leads to a change in dipole moment, due to both the charge transfer and the polarization of the molecules and the gold surface. For sparse coverages (less than 1/3), the induced dipole should not depend much on the distance between molecules. This extra dipole gives a coverage dependent contribution which is included in the adsorption energy reported in Table II. The scaling of this term is inversely proportional to the cube of the intermolecular distance. Using this approach and the data in Table II, we extrapolate the adsorption energy in the dilute limit to be 0.23 eV and the effective dipole moment of the adsorbed monolayer to be 3.35 D. Thus the induced dipole moment in the monolayer is about 0.3 D, a considerably smaller change than found for the AuCNH complex. We also estimate the contribution to the binding that derives from the classical polarization response of the metal surface to the initial dipole on the CNH. We use the point charge model mentioned previously for CNH and assume a classical image potential to arrive at about 0.1 eV. In

TABLE I: Comparison of Au-X complexes, where X is CO, $NH_3$, CNH and $CNCH_3$. All characteristics are calculated with NRLMOL DFT code using both PBE or LDA exchange-correlation potentials. Experimental values of the dipole moments are given in parentheses when available. The X dipole column corresponds to the dipole moment of the isolated molecule X in the case of linear configurations. In the case of a bent configuration, it corresponds to the dipole moment of the ligand X with the geomtery taken from the fully relaxed bent Au-X complex.

| Molecule X | Au-X geometry | Functional | Binding energy, eV | Au-X bond length, $\AA$ | X dipole, D | Au-X dipole, D |
|---|---|---|---|---|---|---|
| CO | linear | PBE | 0.68 | 1.997 | 0.20(0.12)[a] | 1.65 |
| CO | linear | LDA | 1.27 | 1.948 | 0.23 | 1.57 |
| CNH | linear | PBE | 0.93 | 2.002 | 3.09(3.05)[b] | 5.46 |
| CNH | linear | LDA | 1.54 | 1.957 | 3.20 | 5.50 |
| $NH_3$ | linear | PBE | 0.60 | 2.277 | 1.53 | 4.72 |
| $NH_3$ | linear | LDA | 1.07 | 2.188 | 1.54 | 4.89 |
| $CNCH_3$ | linear | PBE | 0.99 | 2.011 | 3.95(3.83)[c] | 6.97 |
| CO | bent | PBE | 0.87 | 2.005 | 0.14 | 0.35 |
| CNH | bent | PBE | 1.04 | 1.989 | 2.69 | 2.89 |
| $CNCH_3$ | bent | PBE | 1.05 | 2.019 | 3.94 | 5.74 |

[a] J. S. Muenter, J. Mol. Spectrosc. **55**, 490 (1975).
[b] G.L. Blackman, R.D. Brown, P.D. Godrey, and H.I. Gunn, Nature **261**, 395 (1976).
[c] S.N. Ghosh, R. Trambarulo, and W. Gordy, J. Chem. Phys. **21**, 308 (1953).

TABLE II: Stabilization energies from WIEN2K calculations for various molecules obtained with GGA-PBE exchange-correlation potential.

| Molecule | Coverage | Site | Stabilization energy, eV |
|---|---|---|---|
| CNH | 1/1 | top | 0.43 |
| CNH | 1/1 | hcp | no adsorption |
| CNH | 1/1 | fcc | no adsorption |
| CNH | 1/1 | bridge | no adsorption |
| CNH | 1/3 | top | 0.18 |
| CNH | 1/3 | hcp | no adsorption |
| CNH | 1/4 | top | 0.20 |
| CNH | 1/4 | hcp | no adsorption |
| $CNCH_3$ | 1/3 | top | 0.22 |
| $CNCH_3$ | 1/3 | hcp | no adsorption |
| CO | 1/3 | top | 0.20 |

comparison to the relatively small extrapolated net adsorption energy, polarization plays a noticeable role.

Given the extra repulsion from the induced dipole, one might have expected the CNH to adopt a bent configuration on the surface. In the radical, this dramatically reduces the dipole, as seen in Table I. This has been investigated by considering small distortions of the CNH away from the vertical a-top structure at 1/3 ML coverage (molecular axis was tilted by 10°, while the geometry of the molecule was otherwise unchanged). Relaxation of this initial configuration results in an essentially vertical structure. Alternatively, we have started from a bent CNH configuration at 1/4 ML coverage (with Au-C bond vertical, CNH molecule positioned as in the bent Au-CNH complex) and relaxed the structure. We find a smooth path back towards the vertical geometry. Evidently the back donation driving force, characterized further in the next section, is weaker in the adsorbed case than in the radical.

In the neutral radical, the net effect of the donor-acceptor bonding is relatively weak due to the partially occupied Au s-orbital. For an Au cation, or a complex which partially withdraws the Au s-electron, the binding can be substantially stronger. Experiments and calculations have been analyzed for a series of ligands bonding to the gold cation[51]. The estimated bond energies for $Au^+CO$, $Au^+NH_3$, and $Au^+CNCH_3$ are 2.1, 3.1 and 3.1 eV respectively. These are all substantially larger than for the corresponding neutral radicals. Furthermore, it is known that isocyanides as well as amines and phosphines passivate gold nanoparticles[15,52,53]. This raises the interesting question of the character of CNH bonding to undercoordinated gold atoms on the surface. To probe this question, we calculated the binding of CNH to an Au adatom using ABINIT. The adatom was relaxed, together with the first full surface layer, in the hcp hollow site of a 4 ML slab with 1/4 coverage. Then the CNH was added to the system and fully relaxed. The final geometry is close to vertical with a reduced Au-C bond length (1.958 $\AA$) and slightly longer C-N bond length (by <0.01 $\AA$) relative to the original a-top geometry. The binding energy is increased by 0.9 eV, relative to the a-top adsorption site on the flat surface. This binding energy refers to an array of CNH molecules in the same unit cell relative to the gold surface including the adatoms. The formation energy of the adatom is not explicitly included since we consider the adatom to be a proxy for undercoordinated gold atoms on the surface of a nanoparticle or

other rough gold surfaces.

Finally, it is well known that the DFT method using the LDA overestimates binding energies. However it is usually expected that general trends are reproduced correctly. Some calculations for the radicals were repeated with the LDA exchange-correlation functional (Table 1). As expected, LDA systematically overestimates binding energies by about 0.6 eV and underestimates the Au-ligand bond lengths. Also, some of the slab calculations of CNH adsorption on Au(111) were repeated using LDA. Adsorption energies calculated with ABINIT for a 1/4 ML coverage are 0.95 eV, 1.09 eV and 1.12 eV for the top, hcp and fcc sites respectively. Similar results are obtained with WIEN2k code for 1/3 ML coverage: 0.80 and 1.03 eV for the top and hcp sites. There is a qualitative difference between the GGA-PBE and LDA results, the GGA being more realistic where experimental tests are available. With GGA the top site is preferred and there is no adsorption at the hcp or fcc sites. With LDA, on the contrary, adsorption at the hcp site is possible and it is energetically favored over adsorption at the top site.

## III. DISCUSSION

We have found that isocyanides selectively bind to the atop site on the flat gold (111) surface, with a small adsorption energy. The C-N bond in the isocyanide is vertical. This binding geometry is consistent with experiments described in the introduction: top site adsorption is observed[15,16] and ellipsometry data indicate vertical orientation of adsorbed isocyanides[19]. At the present there are no measurements of binding energies or saturation coverage of isocyanide molecules on the gold surface for direct comparison to our calculated adsorption energy. The CO molecule, on the other hand, is very well studied. As noted, its electronic structure is similar to that of the CNH molecule. We performed calculations identical to those described above for CO on the gold (111) surface and obtained 0.2 eV for the adsorption energy, in good agreement with previous calculations, but less than the experimental value 0.4 eV[24].

The bonding of both CO and CNH to transition metals is often discussed in terms of the Blyholder picture[26]. Binding involves donation from the filled lone pair on the C into the partially occupied Au s shell together with $2\pi^*$ back donation into the $2\pi^*$ molecular orbital due to interaction with gold $d_{xz}$ and $d_{yz}$. We probe this picture for the bonding of CNH on the flat surface by analyzing the angular character of the local density of states for the adsorbed molecule and the gold slab. The projected density of states (PDOS) for the monolayer adsorbed onto a Au(111) slab at 1/3 coverage in the atop configuration is plotted in Fig. 2 along with the PDOS for a free CNH monolayer and a clean Au(111) slab. Also shown are isosurface plots of selected wavefunctions ($\Gamma$-point) corresponding to certain energy regions in the PDOS of the Au(111)-CNH system.

In the PDOS of the free CNH monolayer several very sharp peaks are observed which can be associated with the molecular orbitals $4\sigma$, $1\pi$, $5\sigma$ and $2\pi^*$ (the last being unoccupied). After adsorption the $4\sigma$ level does not change much and there is no discernable interaction with gold. This is not surprising considering that this level lies well below the bottom of the gold valence band. In contrast, $1\pi$ and $5\sigma$ levels undergo substantial reorganization. The $5\sigma$ state strongly interacts with hybridized $s$ and $d_{z^2}$ orbitals of gold. A localized state is formed below the bottom of the gold valence band. In addition, there is a state of anti-bonding character that can be identified above the occupied gold d-band, but below the Fermi energy (around -1 eV in Fig. 2). These states are very similar to the hybrids that forms in the AuCNH radical. In the radical, the anti-bonding state is half occupied. As a result of the strong $\sigma$ interaction, the $1\pi$ level now lies above $5\sigma$ derived level. The $1\pi$ level interacts with gold $d_{xz}$ and $d_{yz}$ orbitals. This results in two peaks visible in the PDOS at around $-7$ eV and $-5$ eV, of bonding and anti-bonding character respectively, as can be seen from the wavefunction plots. The bonding combination appears to form a localized state just below the bottom of the Au d-bands, while the anti-bonding combination is resonant with the d-bands. Finally, the $2\pi^*$ peak from the CNH derived state density extends somewhat below Fermi energy upon adsorption. The corresponding wavefunction isosurface plot shows that these occupied states are of bonding character between gold p-like states available near the Fermi energy and the CNH $2\pi^*$ orbital. Hence back donation into the $2\pi^*$ orbital contributes to the bonding. Above the Fermi energy, near the center of the resonance, the coupling is weak, but clearly of anti-bonding character to gold $d_{xz}$ and $d_{yz}$ orbitals. This qualitative picture from the PDOS is very similar to previous results for CO adsorbed on the a-top site of gold (111)[24].

It is hard to quantify this analysis of bonding character since the PDOS is calculated using only electron densities inside spheres surrounding the atoms. However, another metric related to bonding trends is the change in C-N bond length upon adsorption on gold. The calculation for the Au-CNH complex shows a C-N bond length of 1.173 $\mathring{A}$ in the straight configuration. Upon full relaxation to the bent configuration, the C-N bond is 1.198 $\mathring{A}$, compared to 1.176 $\mathring{A}$ in the free CNH. This net weakening of the C-N bond upon bending traces to the pseudo Jahn-Teller effect driven by increased occupation of the antibonding $2\pi^*$ orbital. On the other hand, upon adsorption on the Au(111) surface, the calculated C-N bond length is slightly decreased to 1.16 $\mathring{A}$. This contrasts with results for CO adsorption, where the C-O bond length slightly increases upon adsorption[24]. The decrease in C-N bond length suggests slightly less $\pi$ back donation for CNH adsorption on the surface relative to the radical. However, careful study of metal-carbonyl complexes reveals a more complex picture[54]. The final C-N bond length (and the corresponding stretch frequency) reflects

the balance between $\sigma$ bond polarization due to the metal and $\pi^*$ back donation effects. This balance is affected by electrostatics, particularly in the limit of the positively charged carbonyl complex. The positive charge near the C influences the heteropolar C-O $\sigma$ bond, driving it to be more symmetrical and stronger. This also drives an increase in the C-O stretch frequency in the carbonyls. One would expect similar effects on the C-N bond for the CNH case. This is consistent with the observed increase of the C-N stretch frequency in isocyanides adsorbed on gold[15,19].

The initial dipole on the molecule and the induced dipole upon adsorption both play a role. The CNH molecule has a substantial dipole moment, in contrast to the CO molecule. Therefore, in the case of CNH, the binding energy contains some contribution from the polarization energy due to the interaction between the molecular dipole and the gold surface. Our estimates indicated a modest effect (0.1 eV), which is however a non-trivial fraction of the final adsorption energy for an isolated CNH on the flat surface (0.23 eV). Furthermore, the net dipole inhibits formation of a dense film on the surface. The inferred induced dipole on the metal surface is substantially smaller than that found in the isolated Au-CNH radical. This is indicative of less net charge transfer in comparison to the radical. This is not surprising from two points of view. First, the work function of Au(111) (5.31 eV[55]) is smaller than the chemical potential of the Au atom (conventionally the average of the ionization potential and the electron affinity, 5.76 eV[56]). This inhibits the sigma donation from the lone pair. Second, the surface Au s-state is substantially involved in band formation, having nine nearest neighbors. This interferes with hybridization to the lone pair, reducing the net energy gain for the sigma donation process.

The role of charge transfer has been controversial in the analysis of these weakly adsorbed systems and the impact of the hybridization implicit in the Blyholder picture has been debated[24,25,57,58]. Bilic *et al.* argue that the main mechanisms of binding of $NH_3$ to the gold surface are polarization effects and dispersive interactions, not the covalent bonding[25]. In their work on pyridine[57], they find more evidence for charge transfer, but still argue that covalent effects are minimal. A more recent study of pyridine binding to Au[58] analyzed the impact of Au coordination and suggested a more prominent role for hybridization effects. The utility of the Blyholder picture becomes more apparent when examining trends in the binding, e.g. for bonding to different metals[24]. Alternatively, it gives a way to rationalize the trends for the binding of different molecules to the same metal, as described for the Au radicals in Section II. Finally, the sigma donation becomes more prominent for the case of binding to an Au adatom on the surface. We found a large increase in binding energy of CNH compared to the flat surface (0.9 eV). A similar increase was recently reported for $NH_3$ (0.4 eV)[13]. The donor-acceptor binding to the adatom is also enhanced due to the slight positive charge on the Au adatom, similar to the increased binding energy for the Au(I) cation to several ligands[51].

The small calculated value of adsorption energy of isocyanides on the flat gold surface seems to contradict the experimental observation of SAM formation[19]. Two caveats are due here. First, layer formation takes place in a solution. Solvation effects can screen the dipole-dipole interactions and facilitate layer growth from nuclei. Also, a layer of larger molecules (e.g. alkanes) may be more stable than the binding energy of the CNH link moiety would suggest due to attractive inter-molecular interactions between the extended molecules in the layer, e.g. due to dispersive interactions between neighboring alkanes. Second, the presence of undercoordinated Au binding sites at step edges on the surface may facilitate nucleation of the isonitrile layers. We have found that the binding energy to the Au adatom is substantially larger than the binding energy to the top site on the flat surface. This may also account for the binding to powdered gold samples and nanoparticles where undercoordinated Au sites would be common.

Assessing the accuracy of DFT calculations for these weakly bound systems is difficult. The information for the Au radicals was already assessed in Sec. II. In the case of Au-$NH_3$, the GGA Au to $NH_3$ binding energy is smaller than accurate quantum chemistry calculations by about 0.2 eV. Bilic *et al.* studied the binding of $NH_3$ to the gold surface using the GGA with the PW91 exchange-correlation functional, which in this particular case gave an adsorption energy in quantitative agreement with experiment (within 0.1 eV)[25]. For the Au-CO radical, the binding energy is less well established, as discussed in Sec. II. Gajdo *et al.* studied adsorption of CO on (111) surface of various transition and noble metals[24]. In particular, they report results for CO adsorption on Au and Ag surfaces obtained with PW91 and a revised form of the PBE exchange-correlation potentials which has in other cases given more accurate adsorption energies[28]. Adsorption energies were very sensitive to the choice of the functional. Both functionals underestimate adsorption energies. The revised PBE leads to endothermic adsorption while PW91 underestimates the binding energy by about 0.2 eV. The essential mechanisms of binding are very similar for CO and CNH molecules, as it can be seen from the comparison of PDOS pictures. The experience with CO on the flat Au surface suggests that the present DFT calculations may underestimate the binding energy for the CNH case as well. Also, in the CNH case, we have found that the LDA overestimates the radical binding energies and predicts the wrong binding site on the flat surface. The role of dispersion forces in the binding has been debated. The evidence just summarized points to the GGA calculations underestimating the binding energy of CO and CNH on the Au surface. This is consistent with experience in the case of intermolecular interactions for closed shell molecules which are dominated by dispersion forces. The GGA approximations are known to underestimate binding in these cases while LDA over estimates

them[59].

**Acknowledgements** We thank Tao Sun for help with the WIEN2k calculations. We thank J. Davenport for help and for time on computers at the Computational Science Center at Brookhaven National Laboratory. We thank K. K. Likharev for use of Njal supercomputer cluster at Stony Brook. We thank M. R. Pederson and T. Baruah for doing some useful molecular calculations. Work at Stony Brook was supported in part by NSF Grant NIRT-0304122. Work at BNL was supported by U.S. DOE under contract No. DEAC 02-98 CH 10886. Work at Columbia University was supported by the Nanoscale Science and Engineering Initiative of the National Science Foundation under NSF Award Number CHE-0117752 and by the New York State Office of Science, Technology, and Academic Research (NYSTAR).

[1] R.G. Nuzzo and D.L. Allara, J. Am. Chem. Soc. **105**, 4481 (1983).
[2] A. Ulman, Chem. Rev. **96**, 1533 (1996).
[3] F. Schreiber, J. Phys.: Condens. Matter **16**, R881 (2004).
[4] L. Jones, II, J.S. Schumm, and J.M. Tour, J. Organic Chem. **62**, 1388 (1997).
[5] M.A. Reed, C. Zhou, C.J. Muller, T.P. Burgin, and J.M. Tour, Sci. **278**, 252 (1997).
[6] A. Salomon, D. Cahen, S. Lindsay, J. Tomfohr, V.B. Engelkes, and C.D. Frisbie, Adv. Mater. **15**, 1881 (2003).
[7] H. Basch, R. Cohen, and M.A. Ratner, Nano Lett. **5**, 1668 (2005).
[8] G.E. Poirer, Chem. Rev. bf 97, 1117 (1997).
[9] F. Schreiber, Prog. Surf. Sci. **65**, 151 (2000).
[10] D. Fischer, A. Curioni, and W. Andreoni, Lang. **19**, 3567 (2003).
[11] G.S. Tulevski, M.B. Myers, M.S. Hybertsen, M.L. Steigerwald, and C. Nuckolls, Sci. **309**, 591 (2005).
[12] M. Siaj and P.H. McBreen, Sci. **309**, 588 (2005).
[13] L. Venkataraman, J.E. Klare, I.W. Tam, C. Nuckolls, M.S Hybertsen and M. Steigerwald, Nano Lett. **5**, 458 (2006).
[14] S. Lin and R.L. McCarley, Lang. **15**, 151 (1999).
[15] M. J Robertson, R. J. Angelici, Langmuir **10**, 1488, (1994).
[16] K.Shih, R. J. Angelici, Langmuir **11**, 2539 (1995).
[17] S.J. Bae, Ch. Lee, I.S. Choi, Ch.-S. Hwang, M. Gong, K. Kim, and S.-W. Joo, J. Phys. Chem. B **106**, 7076 (2002).
[18] H. S. Kim, S. J. Lee, N. H. Kim, J. K. Yoon, H. K. Park, and K. Kim, Langmuir **19**, 6701 (2003).
[19] J. I. Henderson, S. Feng, T. Bein, and C. P. Kubiak, Langmuir **16**, 6183 (2000).
[20] J. M. Seminario, A.G. Zacarias, and J.M. Tour, J. Am. Chem. Soc. **121**, 411 (1999).
[21] J. Chen, L.C. Calvet, M.A. Reed, D.W. Carr, D.S. Grubisha, D.W. Bennett, Chem. Phys. Lett. **313**, 741 (1999).
[22] J.-O Lee, G. Lientschnig, F. Wiertz, M. Struijk, R.A.J. Janssen, R. Egberink, D.N. Reinhoudt, P. Hadley, and C. Dekker, Nano Letters, **3**, 113 (2003).
[23] Y. Xue and M. A. Ratner, Phys. Rev. B **69**, 085403 (2004).
[24] M. Gajdos, A. Eichler and J. Hafner, J. Phys. Condens. Matter **16**, 1141 (2004).
[25] A. Bilic, J. R. Reimers, N. S. Hush, and J. Hafner, J. Chem. Phys. **116**, 8981 (2002)
[26] G. Blyholder, J. Phys. Chem. **68**, 2772 (1964).
[27] J. P. Perdew, K. Burke, and M. Ernzerhof, Phys. Rev. Letters **77**, 3865 (1996).
[28] B. Hammer, L.B. Hansen, and J.K. Norskov, Phys. Rev. B **59**, 7413 (1999).
[29] S. Kurth, J. P. Perdew, P. Blaha, Int. J. of Quant. Chem. **75**, 889 (1999).
[30] P. J. Feibelman, B. Hammer, J. K. Norskov, F. Wagner, M. Scheffler, R. Stumpf, R. Watwe, and J. Dumesic, J. Phys. Chem. B **105**, 4018 (2001).
[31] A. Gross, Surf. Sci. Rep. **32**, 291 (1998).
[32] The parameterization of Ref.[34] is used with the Abinit slab calculations. Perdew and Wang parametrization[33] is used in NRLMOL and WIEN2k calculations.
[33] J.P. Perdew and Y. Wang, Phys.Rev. B **45**, 13244 (1992).
[34] S. Goedecker, M. Teter, and J. Hutter, Phys. Rev. B **54**, 1703 (1996).
[35] M.R. Pederson and K.A. Jackson, Phys. Rev. B **41**, 7453 (1990); K.A. Jackson and M.R. Pederson, Phys. Rev. B **42**, 3276 (1991).
[36] D. Porezag and M.R. Pederson, Phys. Stat. Solidi (b) **217**, 219 (2000).
[37] D. Porezag and M.R. Pederson, Phys. Rev. A, **60**, 2840 (1999); D. V. Porezag, PhD thesis: http://archiv.tu-hemnitz.de/pub/1997/0025.
[38] P. Blaha, K. Schwarz, G. K. H. Madsen, D. Kvasnicka and J. Luitz, WIEN2k, An Augmented Plane Wave + Local Orbitals Program for Calculating Crystal Properties (Karlheinz Schwarz, Techn. Universitat Wien, Austria), 2001. ISBN 3-9501031-1-2
[39] The ABINIT code is a common project of the Universit Catholique de Louvain, C. I., and other contributors. URL http://www.abinit.org.
[40] X. Gonze, J.M. Beuken, R. Caracas, F. Detraux, M. Fuchs, G.M. Rignanese, L. Sindic, M. Verstraete, G. Zerah, F. Jollet, M. Torrent, A. Roy, M. Mikami, P. Ghosez, J.Y. Raty, and D.C. Allan, Computational Materials Science **25**, 478 (2002).
[41] C. Hartwigsen, S. Goedecker, and J. Hutter, Phys. Rev. B **58**, 3641 (1998).
[42] N. Troullier and J.L. Martins, Phys. Rev. B **43**, 8861 (1991).
[43] M. Fuchs and M. Scheffler, Computer Physics Communications **119**, 67 (1999).
[44] P. E. Blochl, O. Jepsen and O. K. Andersen, Phys. Rev B **49**, 16223 (1994).
[45] N.A. Lambropoulos, J.R. Reimers, and N.S. Hush, J. Chem. Phys. **116**, 10277 (2002).
[46] T.K. Dargel, R.H. Hertwig, W. Koch, and H. Horn, J. Chem. Phys. **108**, 3876 (1998).
[47] P. Schwerdtfeger and G.A. Bowmaker, J. Chem. Phys. **100**, 4487 (1994).
[48] B. Liang and L. Andrews, J. Phys. Chem. A **104**, 9156 (2000).
[49] F. Mendizabal, Organometallics **20**, 261 (2001).
[50] X. Wu, L. Senapati, S.K. Nayak, A. Selloni, and M. Hajaligol, J. Chem. Phys. **117**, 4010 (2002).
[51] D. Schroder, H. Schwarz, J. Hrusak, and P. Pyykko, Inorg. Chem., **37**, 624 (1998).
[52] D. V. Leff, L. Brandt, and J. R. Heath, Langmuir **12**, 4723

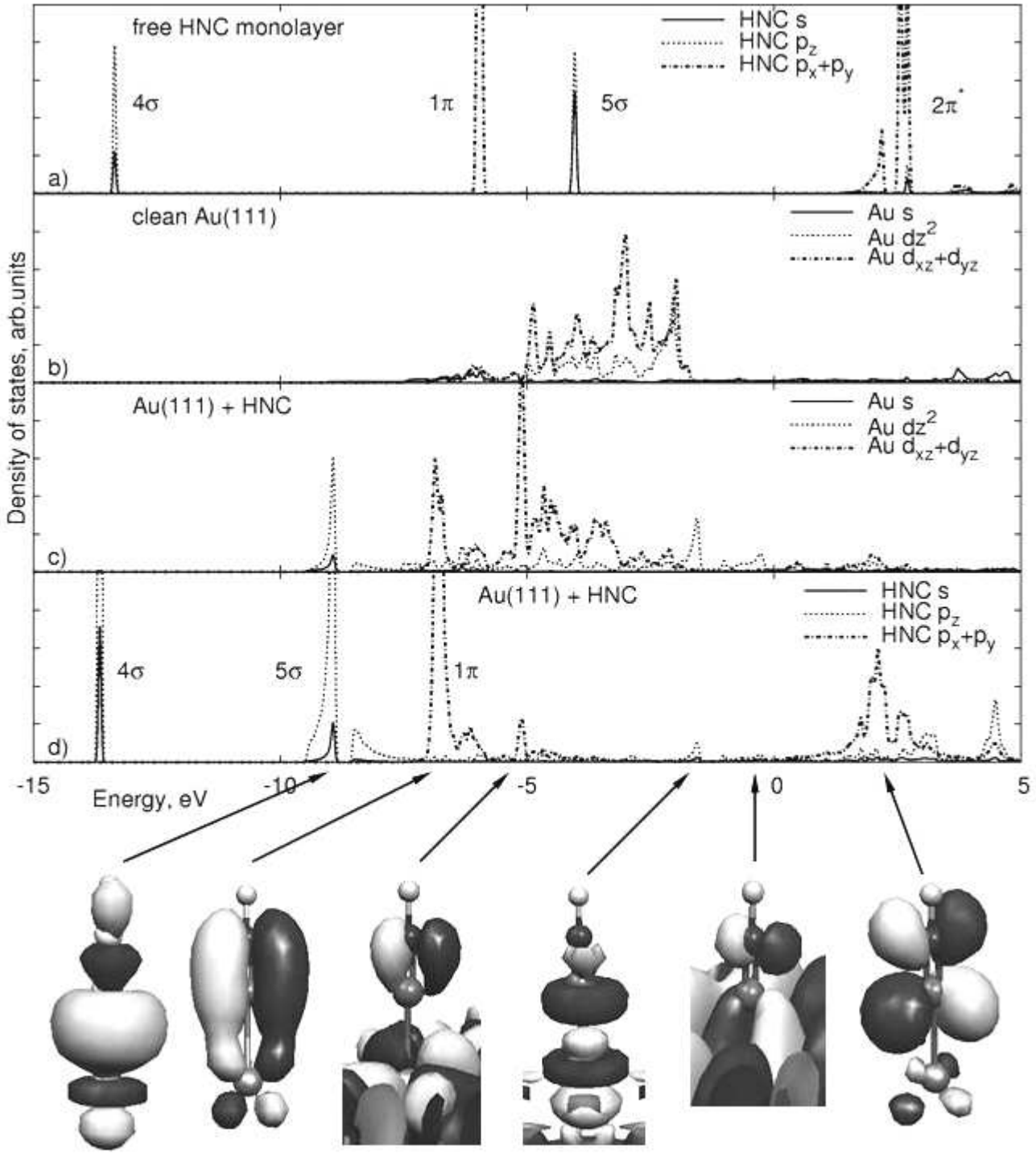


FIG. 2: Projected density of states onto: (a) the HNC molecule in free-standing monolayer; (b) the surface Au atom in the clean Au(111) slab; (c) the Au atom bound to the molecule in the Au(111)-CNH system (1/3 ML, atop site); (d) the HNC molecule in the Au(111)-CNH system. Panel (e) shows isosurface plots of selected wavefunctions (at Γ-point) of the Au(111)-CNH system at energies indicated by the arrows.

(1996).
[53] W. W. Weare, S. M. Reed, M. G. Warner, and J. E. Hutchison, J. Am. Chem. Soc. **122**, 12890 (2000).
[54] A.J. Lupinetti, S. Fau, G. Frenking, and S.H.Strauss, J. Phys. Chem. A **101**, 9551 (1997).
[55] H. B. Michaelson, J. Appl. Phys. **48**, 4729 (1977).
[56] J. M. Dyke, N. K. Fayad, A. Morris, and I. R. Trickle, J. Phys. B **12**. 2985 (1979); G. Gantefor, S. Kraus, and W. Eberhardt, J. Electron Spectrosc. Relat. phenom. **88**, 35 (1998).
[57] A. Bilic, J.R. Reimers, and N.S. Hush, J. Phys. Chem. B **106**, 6740, (2002).
[58] R. Stadler, K.S. Thygesen, and K.W. Jacobsen, Phys. Rev. B **72**, 241401(R) (2005).
[59] E.J. Meijer and M. Sprik, J. Chem. Phys. **105**, 8684 (1996).